Applied Laser Technology
Vol. 28, No.3,July (2021), pp.01–05

Electrical Power Traction Line Fault Localization

CH SWAPNA[1] , AKURATHI SRINIVASA RAO[2]
Assistant professor[1,2]
DEPARTMENT OF ELECTRICAL AND ELECTRONICS ENGINEERING
P.B.R.VISVODAYA INSTITUTE OF TECHNOLOGY & SCIENCE
S.P.S.R NELLORE DIST, A.P , INDIA , KAVALI-524201

abstract

This study provides an abstract discussion of fault localization strategies for single-end direct power supply networks used in electrical traction. With the use of the current and voltage value at the measuring end of the electrical traction line and the system's distributed parameter model, the location of the short-circuit problem may be determined. Factors such as transient resistance, locomotive location, and load are examined in relation to fault localization. The simulation tests are performed using the MATLAB simulation program. The efficiency of the suggested algorithms is shown by simulation results.

Key words :

Fault localization in a traction system; steady-state resistance analysis; analysis of resistance

Introduction

Due to the importance of safety, dependability, stability, and economy in railway operations, pinpoint fault identification in electrical traction network systems is a topic of intense research [1,2]. Because of the traction system's unique characteristics—its power supply structure, operating mode, and traction load—fault distance assessment is notoriously difficult to perform. The sooner and more easily the system can be restored, the more precisely the defect may be detected. It may alleviate the burden on fault patrol, save maintenance downtime, cut customer complaints, and boost protection effectiveness. The field of fault distance measuring in power system transmission and distribution lines (including cable) has made great strides in recent years. Wire short-circuit faults are the most common kind of fault, while contact network cut-line grounding faults and different-phase short-circuit faults also occur. The problem in a traction system with a single power source is often realized as a grounding occurrence in the contact network.

There is a momentary increase in resistance between the fault and ground when a fault occurs. Because the grounding resistance and the arc resistance created during the short-circuit period are independent of the fault point's location, it is a random variable. The conductivity of the wire material, the space structure, and the ground dirt substance all often affect the short-circuit reactance. After the contact network is built, the basic line reactance is calculated, which is independent of the methods used to create a short circuit and provide electricity. Fault detection techniques may be categorized as either "active" or "passive." The S signal injection strategy is one way to pinpoint the location of a defect in an active pattern without cutting power to the system. However, if electric-arc phenomenon occurs intermittently at the grounding point of the connection, the injection signal cannot

be continuously sent through the electrical line, leading to further complications in pinpointing the exact position of the problem. The expense and complexity of the detection process rise if the fault location is situated off-line and additional direct current high voltage must be applied to maintain the shooting status at the ground position. Passive fault location, on the other hand, is accomplished by the signals acquired from the measurement terminals at the moment of the fault occurrence without the need of any auxiliary tools. It's convenient for immediate use. Therefore, passive fault location methods, such as the impedance technique [3-6] and the traveling wave method [7-9], are the direction of development for fault location in distribution power networks. The algorithms of fault finding may be broken down into single-terminal and double-terminal techniques [10,11] based on the information sources from the measurement perspective.

Measuring Fault Distance Algorithms

Fault-Location-Determination Methods Ignoring Locomotives

Figure 1 depicts a fault traction system with a short circuit. Traction substation may be modelled as an impedance Zs power source Es. Traction line length is l, starting and ending points are m and n, respectively.

The distance from the power plant to the location of the fault is denoted by lf, where f is the fault point. The traction network system's energy transfer via the contact network and the track loop may be described by the transmission line equation. As illustrated in Figure 3, an analogous circuit model of the damaged traction network system is shown. At the site of the fault, the transient resistance is denoted by the symbol Rf. The locomotive may be seen of as a source of direct current (the infinitive of an empty load) or a fixed impedance Zt. In this section, the locomotive is modeled as an infinitely resistive current source. In this case, let's suppose that the resistance, inductance, and capacitance of electrical traction lines are normally distributed, with per-unit-length Energies 2012, 5 5005 values of R0, L0, and C0. Here, we disregard the ground inductance G0. Table 1 [24] displays the values for the transmission line parameters.

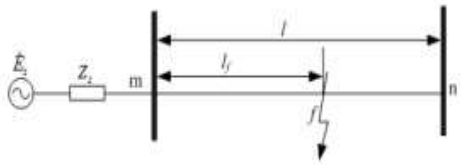

Figure 1. The faulted traction network system.

Table 1. The electrical parameters of the traction line

Parameter	Value
R_0/(Ω/km)	0.1–0.3
L_0/(mH/km)	1.4–2.3
C_0/(nF/km)	10–14

Lumped Transmission Line Parameter Condition

The short-circuit fault model with single-ended power supply and lumped transmission line parameters is shown in Figure 2. Zl is the line impedance, and x is the per-unit-length from the measurement m-point to the fault, x = lf l . The voltage at the measurement m-point is expressed as,

$$\dot{U}_m = \dot{I}_m \cdot x \cdot Z_l + \dot{I}_f \cdot R_f$$

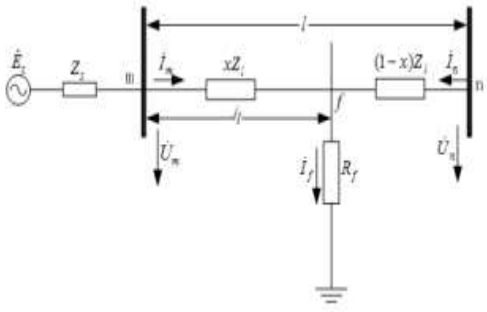

Figure 2. The faulted traction network system.

Since it is an open-circuit model,

$$\dot{I}_m = \dot{I}_f, \text{ then } \dot{U}_m = \dot{I}_m \cdot x \cdot Z_l + \dot{I}_m \cdot R_f.$$

As the Equation (1) is a complex form, it can be derived into real part and imaginary part functions, therefore,

$$\mathrm{Im}(\dot{U}_m) = \mathrm{Im}(I_m Z_l) \cdot x + \mathrm{Im}(\dot{I}_m) \cdot R_f$$

$$\mathrm{Re}(\dot{U}_m) = \mathrm{Re}(I_m Z_l) \cdot x + \mathrm{Re}(\dot{I}_m) \cdot R_f$$

Multiply Equation (2a) by Re(˙Im) and Equation (2b) by Im(˙Im), and then subtract both side of the equations, it gives.

$$x = \frac{\mathrm{Re}(\dot{I}_m)\,\mathrm{Im}(\dot{U}_m) - \mathrm{Im}(\dot{I}_m)\,\mathrm{Re}(\dot{U}_m)}{\mathrm{Re}(\dot{I}_m)\,\mathrm{Im}(\dot{I}_m Z_l) - \mathrm{Im}(\dot{I}_m)\,\mathrm{Re}(\dot{I}_m Z_l)}$$

Using the voltage and current measured at the m-end under the effect of the fault resistance component Rf, the fault location may be calculated using Equation (3).

Calculation Outcomes

The following simulated experiments make use of the setup shown in Figure 1. The electrical traction system receives power from a single phase of AC current at an industrial frequency. The electrical substation typically converts the three-phase 110 kV high voltage to the single-phase 27.5 kV that is used by each traction system. Therefore, Es = 27.5 kV with impedance Zs = 0.245 + j1.055 was used for the traction power sources in the trials. The length of the traction line is 30 kilometres. Table 1 summarizes the transmission line characteristics that define a traction line: R0 = 0.232 /km, L0 = 1.64 mH/km, and C0 = 10.5 nF/km. The input is the first cycle's worth of voltage samples at a sampling rate of 200 kHz. Then, the fault distance lf is solved using Equations (3), (15), (24) and (29), where M1, M2, M3, and M4 are four fault distance estimate techniques.

By plugging the estimated fault distance into the following calculation and comparing it to the actual fault distance,

$$e_{l_f} = \left| \frac{l_{f-calculated} - l_f}{l} \right|$$

where lf−calculated is the calculated fault distance from the developed algorithms and lf is the actual fault point in the system.

Table 2 lists the results with three approaches: Reactance, Lumped parameter (M1) and Distributed parameter (M2) for fault distance calculation under various fault transient resistances and fault positions and zero load. It shows that the results derived from Reactance approach are the same as those derived from (M1). It is true since they share the same theory only with different calculation procedures. Compared the results from (M1) and (M2), the estimated fault distance from (M2) is more accurate since the transmission line characteristics are considered in the algorithms.

Table 2. The lf estimation with different fault transient resistance Rf and Zt = ∞.

R_f (Ω)	l_f (km)	Fault distance measurement and results					
		Reactance		Lumped para (M1)		Distributed para (M2)	
		Calculated	e_{l_f} (%)	Calculated	e_{l_f} (%)	Calculated	e_{l_f} (%)
0	6	5.9691	0.1030	5.9691	0.1030	6.0001	0.0003
	14	13.9288	0.2373	13.9288	0.2373	14.0013	0.0043
	26	25.8733	0.4223	25.8733	0.4223	26.0083	0.0277
50	6	5.4884	1.7053	5.4884	1.7053	6.0169	0.0563
	14	13.4355	1.8817	13.4355	1.8817	14.0258	0.0860
	26	25.3421	2.1930	25.3421	2.1930	26.0255	0.0850
100	6	4.0522	6.4927	4.0522	6.4927	6.03376	0.1125
	14	11.9867	6.7110	11.9867	6.7110	14.0503	0.1677
	26	23.8542	7.1527	23.8542	7.1527	26.0427	0.1423

The influence of the locomotive Zt and fault transient resistance Rf when the fault distance is calculated from (M3) are discussed. Tables 3–6 demonstrate that the accuracy of lf−calculated is related to the magnitude of Rf , that is to say, the fault type. With the growing of the fault transient resistance, the fault distance algorithms (M3) could results in failure. However, the algorithm described in (M2) is not affected by the Rf , since the locomotive is not considered. Although better fault distance calculation can be obtained from algorithm of M2 in ideal status, the effect of the locomotive in actual operational environment can not be omitted due to uncertain factors.

Table 3. The lf estimation with various locomotive load when lt = 5 km, Rf = 0 Ω

Locomotive load Z_t	Fault distance $l_f(km)$	Fault distance measurement and results			
		Reactance		New algorithm (M3)	
		Calculated	e_{l_f} (%)	Calculated	e_{l_f} (%)
$Z_t = 54$	6	5.9600	0.1333	6.0473	0.1579
	14	13.1838	2.7207	14.4146	1.3820
	26	21.8284	13.9052	26.9293	3.0978
$Z_t = 60$	6	5.9609	0.1303	6.0424	0.1415
	14	13.2589	2.4703	14.3728	1.2427
	26	22.2239	12.5870	26.8403	2.8012
$Z_t = 66$	6	5.9616	0.1278	6.0384	0.1283
	14	13.3204	2.2653	14.3387	1.1291
	26	22.5508	11.4973	26.7670	2.5567

Table 4. The lf estimation with various locomotive load when lt = 5 km, Rf = 20 Ω

Locomotive load Z_t	Fault distance $l_f(km)$	Fault distance measurement and results			
		Reactance		New algorithm (M3)	
		Calculated	e_{l_f} (%)	Calculated	e_{l_f} (%)
$Z_t = 54$	6	5.4592	1.8027	6.0499	0.1666
	14	9.4120	15.2930	14.564	1.8830
	26	14.4751	38.4163	27.2918	4.3060
$Z_t = 60$	6	5.4868	1.7105	6.0445	0.1485
	14	9.6849	14.3835	14.4936	1.6453
	26	15.1344	36.2185	27.1305	3.7683
$Z_t = 66$	6	5.5112	1.6293	6.0405	0.1352
	14	9.9272	13.5760	14.4385	1.4617
	26	15.7247	34.2510	27.0048	3.3493

Table 5. The lf estimation with various locomotive load when lt = 5 km, Rf = 50 Ω.

Locomotive load Z_t	Fault distance	Fault distance measurement and results			
		Reactance		New algorithm (M3)	
	$l_f(km)$	Calculated	e_{l_f} (%)	Calculated	e_{l_f} (%)
$Z_t = 54$	6	5.1116	2.9613	6.0540	0.1802
	14	7.1568	22.8107	14.7998	2.6660
	26	9.9079	53.6401	27.8583	6.1944
$Z_t = 60$	6	5.1260	2.9133	6.0478	0.1594
	14	7.3888	22.0371	14.6809	2.2697
	26	10.4525	51.8250	27.5800	5.2667
$Z_t = 66$	6	5.1394	2.8684	6.0437	0.1460
	14	7.6073	21.3089	14.5921	1.9738
	26	10.9677	50.1077	27.3710	4.5700

Table 6. The lf estimation with various locomotive load when lt = 5 km, Rf = 100 Ω

Locomotive load Z_t	Fault distance	Fault distance measurement and results			
		Reactance		New algorithm (M3)	
	$l_f(km)$	Calculated	e_{l_f}(%)	Calculated	e_{l_f} (%)
$Z_t = 54$	6	4.8602	3.7990	6.0613	0.2043
	14	5.8106	27.2978	15.2187	4.0625
	26	7.1359	62.8801	28.868	9.5600
$Z_t = 60$	6	4.8440	3.8533	6.0535	0.1785
	14	5.9320	26.8932	15.0100	3.3667
	26	7.4535	61.8215	28.3701	7.9003
$Z_t = 66$	6	4.8279	3.9069	6.0493	0.1646
	14	6.0521	26.4929	14.8594	2.8647
	26	7.7684	60.7720	28.0080	6.6936

In Table 7, the fault distance is estimated when the locomotive is regarded as a constant power load. When the fault transient resistance is 0, the obtained fault distance from M4 is more accurate. However, if the fault transient resistance Rf is increasing, the accuracy of the calculated fault distance will decrease gradually.

Table 7. The lf calculation when locomotive is a constant power load.

Transient resistance	Fault distance	Fault distance measurement and results			
		Reactance		New algorithm (M4)	
$R_f(\Omega)$	$l_f(km)$	Calculated	e_{l_f}(%)	Calculated	e_{l_f} (%)
0	6	5.9690	0.1030	5.8899	0.3670
	14	13.3714	2.0953	14.0058	0.0193
	26	22.2777	12.4077	25.7049	0.0193
50	6	4.7854	4.0487	6.66124	2.2010
	14	11.5264	8.2453	15.2937	4.3123
	26	19.4371	21.8763	27.3500	4.5000
100	6	3.7350	7.5500	7.6162	5.3873
	14	9.9142	13.6193	16.8078	9.3593
	26	16.9867	30.0443	29.2622	10.8740

It's important to keep in mind that the aforementioned simulated experimental findings only apply to perfect test conditions. Due to limitations imposed by the test conditions, this study does not include any results from actual field experiments. Many reasons, including fault transient resistance and changes in electrical line characteristics, may lead to the failure of fault site identification in real-world fault distance measurement for electrical traction systems. In the event that the currently employed fault location algorithm is unable to pinpoint

the precise location of the problem, other algorithms already present within the measuring device can be used to generate additional estimation results, increasing the likelihood that at least one of these results will be relatively close to the true fault location. Additionally, the accuracy of the predicted fault site may be improved by comparing the outcomes from many fault estimating techniques. Therefore, alternative measuring techniques should also be implemented to enhance the fault location, and the predictions of the fault distance should be compared taking into account the real complex operating environment.

conclusion

In this research, we investigate numerous fault distance estimate techniques in the context of a single-end direct power supply electrical traction system, with an emphasis on the failure stable state features. The paper's suggested algorithms are straightforward and easy to implement. Knowing the voltage and current at the transmission line's measuring terminal allows one to calculate the fault's location. The new algorithms also take into account the resistance of locomotives and fault transients, unlike the conventional impedance technique. The predicted position of the fault, based on the simulation findings, is quite precise. However, several external variables, such as poor weather and wire aging, may create measurement inaccuracies when fault distance is measured on the spot. Therefore, different measuring techniques should be helped to compare the predicted fault distance taking into account the real complex operating environment in order to increase the accuracy of the fault location.

References

[1]. Ekici, S. Support vector machines for classification and locating faults on transmission lines. Appl. Soft Comput. 2012, 12, 1650–1658.

[2]. Robert, S.; Stanislaw, O. Accurate fault location in the power transmission line using support vector machine approach. IEEE Trans. Power Syst. 2004, 19, 979–986.

[3]. De Morais Pereira, C.E.; Zanetta, L.C., Jr. An optimisation approach for fault location in transmission lines using one terminal data. Int. J. Electr. Power Energy Syst. 2007, 29, 290–296.

[4]. Takagi, T.; Yamakoshi, Y.; Yamaura, M. Development of a new type fault locator using the one-terminal voltage and current data. IEEE Trans. PAS 1982, 101, 2892–2898.

[5]. Waikar, D.L.; Chin, P.S.M. Fast and accurate parameter estimation algorithm for digital distance relaying. Electr. Power Syst. Res. 1998, 44, 53–60.

[6]. Zivanovic, R. An application of global sensitivity analysis in evaluation of transmission line fault-locating algorithms. Procedia Soc. Behav. Sci. 2010, 2, 7780–7781.

[7]. Avdakovic, S.; Nubanovic, A.; Kusljugic, M.; Kusljugicb, M.; Musica, M. Wavelet transform applications in power system dynamics. Electr. Power Syst. Res. 2012, 83, 237–245.

[8]. Bernadi, A.; Leonowicz, Z. Fault location in power networks with mixed feeders using the complex space-phasor and hilbert-huang transform. Electr. Power Energy Syst. 2012, 42, 208–219.

[9]. Jung, H.; Park, Y.; Han, M.; Leea, C.; Parka, H.; Shinb, M. Novel technique for fault location estimation on parallel transmission lines using wavelet. Electr. Power Energy Syst. 2007, 29, 76–82.

[10]. Firouzjah, K.G.; Sheikholeslami, A. A current independent method based on synchronized voltage measurement for fault location on transmission lines. Simul. Model. Pract. Theory 2009, 17, 692–707.

[11]. Guobing, S.; Jiale, S.; Ge, Y. An accurate fault location algorithm for parallel transmission lines using one-terminal data. Electr. Power Energy Syst. 2009, 31, 124–129.

[12]. Liao, Y. Transmission line fault location algorithms without requiring Line parameters. Electr. Power Compon. Syst. 2008, 36, 1218–1225.

[13]. Lin, X.; Weng, H.; Wang, B. A generalized method to improve the location accuracy of the single-ended sampled data and lumped parameter model based fault locators. Electr. Power Energy Syst. 2009, 31, 201–205.

[14]. Funk, A.T.; Malik, O.P. Impedance estimation including ground fault resistance error correction for distance protection. Electr. Power Energy Syst. 2000, 22, 59–66.

[15]. Jiale, S.; Qi, J. An accurate fault location algorithm for transmission line based on R-L model parameter identification. Electr. Power Syst. Res. 2005, 76, 17–24.

[16]. Lian, B.; Salama, M.M.A.; Chikhani, A.Y. A time domain differential equation approach using distributed parameter line model for transmission line fault location algorithm. Electr. Power Syst. Res. 1998, 46, 1–10.

[17]. Mardiana, R.; Motairy, H.A.; Su, C.Q. Ground fault location on a transmission line using high-frequency transient voltages. IEEE Trans. Power Deliv. 2011, 26, 1298–1299.

[18]. Jiale, S.; Guobing, S.; Xu, Q.; Chao, Q. Time-domain fault location algorithm for parallel transmission lines using unsynchronized currents. Electr. Power Energy Syst. 2006, 28, 253–260.

[19]. Jiang, Z.; Miao, S.; Xu, H.; Liu, P.; Zhang, B. An effective fault location technique for transmission grids using phasor measurement units. Electr. Power Energy Syst. 2012, 42, 653–660.

[20]. Cheng, W.; Xu, G.; Mu, L. A novel fault location algorithm for traction network based on distributed parameter line model. Proc. CSU-EPSA 2005, 17, 63–66.